Rapamycin-induced autophagy attenuates hormone-imbalance-induced chronic non-bacterial prostatitis in rats via the inhibition of NLRP3 inflammasome-mediated inflammation

JINGXIAO LU[1*], YANG SU[1*], XIANGUO CHEN[2], YUAN CHEN[3], PENGCHENG LUO[4], FANGYOU LIN[1] and JIE ZHANG[1,4]

[1]Department of Urology, Renmin Hospital of Wuhan University, Wuhan, Hubei 430060;
[2]Department of Urology, The First Affiliated Hospital of Anhui Medical University, Hefei, Anhui 230032;
[3]Department of Clinical Laboratory, Children and Women Hospital of Edong Health Group;
[4]Department of Urology, Huangshi Central Hospital, Hubei Polytechnic University, Huangshi, Hubei 435000, P.R. China

Received March 10, 2018; Accepted October 31, 2018

DOI: 10.3892/mmr.2018.9683

Abstract. Chronic non-bacterial prostatitis (CNBP) is a common urinary disease and no standard treatments are available at present. Although autophagy serves an important role in a variety of chronic diseases, its role in CNBP is yet to be fully elucidated. Therefore, the present study aimed to investigate the effects of rapamycin-induced autophagy on CNBP by establishing a rat model. In the present study, a total of 30 male Sprague-Dawley rats were randomly divided into three groups (n=10 per group): i) Control, in which rats underwent a sham operation; ii) the model (CNBP), in which rats were castrated and administered 17β-estradiol (0.25 mg/kg via subcutaneous injection) for 30 consecutive days; and iii) rapamycin treatment, in which rats were employed in accordance with the CNBP model, but also received a daily intraperitoneal injection of rapamycin (1 mg/kg) from the 16th day post-surgery for 15 days. Alterations in histology and the levels of autophagy-associated markers, and components of the NLRP3 inflammasome, were measured in the prostate tissues of the rats. The levels of molecules located further downstream of the NLRP3 inflammasome pathway, including interleukin (IL)-1β and IL-18, were also measured. The results demonstrated that, compared with the control group, increased infiltration levels of inflammatory cells and glandular epithelial degeneration were observed in the prostate tissues of rats with CNBP. Furthermore, a significant increase in the concentration of IL-1β and IL-18 in the serum, as well as the increased expression levels of NLRP3, ASC and caspase-1 in prostate tissues were also observed. In addition, reductions in the number of autophagosomes and the expression levels of autophagy-associated, including microtubule-associated protein 1 light chain 3β (LC3B) and Beclin 1, were also detected in the CNBP group; however, treatment with rapamycin reversed these effects. Collectively, the findings of the present study indicated that the NLRP3 inflammasome-mediated inflammatory response was activated by a hormonal imbalance in the prostate glands of rats; however, these effects may be suppressed via rapamycin-induced autophagy.

Correspondence to: Professor Jie Zhang, Department of Urology, Renmin Hospital of Wuhan University, 99 Zhang Zhi-dong Road, Wuhan, Hubei 430060, P.R. China
E-mail: whuzhangjie@163.com

*Contributed equally

Key words: autophagy, chronic prostatitis, inflammasomes, cytokines, inflammation

Introduction

Prostatitis is the most common type of urinary disease in males <50 years of age (1) and has a prevalence ranging from 2-9% in the general male population (2). It was reported that ≤50% of males may suffer from chronic prostatitis at a certain stage of their life (3). According to the National Institutes of Health, prostatitis is divided into four categories: Acute bacterial prostatitis, chronic bacterial prostatitis, chronic prostatitis (CP)/chronic pelvic pain syndrome and asymptomatic inflammatory prostatitis (4). As a common type of prostatitis, chronic non-bacterial prostatitis (CNBP; also termed CP) is difficult to diagnose; the long-term therapeutic effects resulting from the routine use of antibiotics and α-blockers have not been reported (5), which leads to a high recurrence rate and a low curative rate for CNBP. Furthermore, CNBP may cause male infertility and sexual dysfunction (6). In addition, continual and recalcitrant inflammation in the prostate has been reported to be associated with prostate cancer and benign prostatic hyperplasia (BPH) (7,8). As CP has a high incidence rate and is associated with numerous hazards, including male infertility and sexual dysfunction, the disease presents a great challenge for clinicians.

Nucleotide oligomerization domain (NOD)-like receptors (NLRs) belong to the family of pattern recognition receptors that recognize pathogen-associated molecular patterns (PAMPs), as well as host-derived danger-associated molecular patterns (DAMPs). NOD-like receptor family pyrin domain-containing proteins (NLRPs) serve a critical role in the innate and adaptive immune responses, and are involved in the development of chronic inflammatory diseases, including cryopyrin-associated periodic syndromes, gout, atherosclerosis and type 2 diabetes (9). As the most widely studied inflammasome, the NLRP3 inflammasome is composed of NOD-like receptor protein 3 (NLRP3), apoptosis-associated speck-like protein containing a caspase recruitment domain (ASC) and caspase-1 (10). NLRP3 interacts with ASC to activate caspase-1, and activated caspase-1 subsequently upregulates the production of proinflammatory cytokines, including interleukin (IL)-1β and IL-18, leading to tissue injury (11).

Autophagy is an evolutionarily conserved cellular process involved in the isolation and degradation of cytosolic macromolecules, damaged organelles and several pathogens, and senescence (12,13). Autophagy is maintained at low levels under physiological conditions; however, it may be induced by nutrient deprivation, mitochondrial damage and pharmacological inhibitors of mammalian target of rapamycin (mTOR), such as rapamycin (14). It was previously reported that the inhibition of autophagy promoted antigen-presenting cells to process and secrete IL-1β in an NLRP3- and Toll/IL-1 receptor-domain-containing adaptor-inducing interferon-β-dependent manner (15). Downregulation of autophagy induced by knockdown of autophagy-related 7 (Atg7) or Atg16L1 promoted the notably enhanced secretion of IL-1β and IL-18 in response to lipopolysaccharide and other PAMPs (16). These studies suggested that autophagy may directly or indirectly inhibit IL-1β and IL-18 secretion, and that this process may be associated with the NLRP3 inflammasome. Our previous study demonstrated that the level of autophagy was suppressed, and the expression levels of cytokine IL-1β, a molecule located downstream of the NLRP3 inflammasome pathway, was significantly increased in CNBP rats (17); however, the association between autophagy and the NLRP3 inflammasome in CNBP is yet to be investigated.

Therefore, the present study employed rapamycin, a well-reported inhibitor of mTOR that serves a key role in autophagy, was used to assess the effects of autophagy on NLRP3 inflammasome-mediated inflammation in the prostate via a rat model in order to determine the mechanism underlying the pathogenesis of CNBP.

Materials and methods

Establishment of the CNBP rat model. A total of 30 male Sprague-Dawley rats (6 weeks old) weighing 250±20 g were purchased from the Center of Experimental Animals of Wuhan University (Wuhan, China). All rats were housed in a specific pathogen-free facility at a constant ambient temperature (22±2˚C) and humidity (50±10%) under a 12 h light/dark cycle, with free access to sterile water and regular chow. The present study was approved by the Ethics Committee for Animal Experiments of Renmin Hospital of Wuhan University (approval no. WDRM-20170709). All animal welfare and experimental procedures were performed in accordance with the guidelines approved by the Care and Use of Laboratory Animals of Renmin Hospital of Wuhan University. The rats were randomly divided into three groups (n=10 per group) on the basis of experimental requirements and anesthetized via inhalation of 1-3% isoflurane prior to surgery: i) Control group, in which sham surgery was performed on each of the rats; ii) CNBP group, in which the rats were castrated and then subcutaneously injected with 17β-estradiol (0.25 mg/kg; Sigma-Aldrich; Merck KGaA, Darmstadt, Germany) for 30 consecutive days; and iii) rapamycin-treated group, in which the rats also received a daily intraperitoneal injection of rapamycin (1 mg/kg; Sigma-Aldrich; Merck KGaA) (18,19) from the 16th day post-surgery for a total of 15 days, based on the same model as the CNBP rats. All rats were sacrificed via an overdose of isoflurane inhalation prior to further analysis. The experimental outline of the present study is presented in Fig. 1.

Histological examination. The prostates were removed and fixed in 10% neutral buffered formalin for 24 h at room temperature. All tissue samples were dehydrated, embedded in paraffin and cut into 4-μm sections. The sections were then stained with hematoxylin and eosin (H&E) for 3-5 min at room temperature, and subsequently examined under a light microscope (magnification, x200; Olympus Corporation, Tokyo, Japan), with 10 areas randomly selected from each section to quantitatively assess the extent of CNBP.

The inflammation scoring criteria used in the present study were as follows. Extent of inflammatory cell infiltration: Low, only normal cells or few inflammatory cells (0 points); mild, a small degree of inflammatory cell infiltration (3 points); severe, a high degree of inflammatory cell infiltration (6 points). Gland lumen: Normal, a single columnar or cubic gland epithelium (0 points); mild, a slightly smaller gland lumen detected (2 points); severe, markedly smaller or occluded gland lumen (4 points). Glandular secretion: Normal, a notable degree of deep-pink staining (0 points); mild, slightly reduced pink staining (2 points); and severe, decreased luminal secretion or no secretion with weak or no pink staining (4 points). Fibrous tissue hyperplasia: Normal, a notably small degree or no fibrous hyperplasia (0 points); mild, a small degree of fibrous hyperplasia (3 points); severe, a high degree of fibrous hyperplasia (6 points). The total score was calculated as the sum of the aforementioned criteria.

Enzyme-linked immunosorbent assay (ELISA) analysis. The blood samples were collected from the inferior vena cava and centrifuged at 4˚C, 2,000 x g for 10 min. The separated serum was used for biochemical analysis. The serum levels of IL-1β (cat. no. EK0393) and IL-18 (cat. no. EK0592) were measured using a rat ELISA kit purchased from Wuhan Boster Biological Technology, Ltd. (Wuhan, China). The absorbance at 450 nm was measured on a microplate reader (BioTek Elx9808; BioTek Instruments, Inc., Winooski, VT, USA).

Immunohistochemistry (IHC) analysis. Paraffin-embedded prostatic sections were deparaffinized in xylene for 15 min, rehydrated with descending alcohol solutions, and heated at 105˚C for 10 min in citric acid buffer (0.01 M, pH 6.0) for antigen

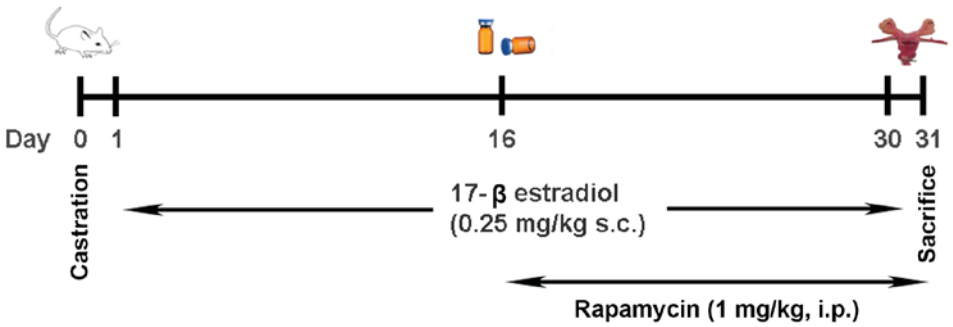

Figure 1. Schematic representation of the experimental design of the present study.

retrieval. The slides were subsequently rinsed with PBS for 10 min, and then transferred to 3% hydrogen peroxide for 5 min at room temperature to block endogenous peroxidase activity. After an additional wash with PBS for 5 min, the sections were blocked with blocking buffer (OriGene Technologies, Inc., Beijing, China) for 1 h at room temperature prior to incubation with primary antibodies against NLRP3 (cat. no. ab214185), ASC (cat. no. ab47092), microtubule-associated protein 1 light chain 3β (LC3B; cat. no. ab48394; all at 1:300 dilution; Abcam, Cambridge, UK) and caspase-1 (cat. no. ab108362; 1:50; Abcam) for 60 min at room temperature, and subsequently biotin-conjugated goat-anti-rabbit immunoglobulin G (IgG) secondary antibody (cat. no. TA130016; 1:200; OriGene Technologies, Inc.) was added to each section and incubated at 37˚C for 50 min. The SP9000 IHC immunochemistry kit (OriGene Technologies, Inc.) and 3,3'-diaminobenzidine (SK-4100; Vector Laboratories, Inc., Burlingame, CA, USA) were used according to the manufacturer's protocols to detect the immune complexes in the prostate tissues. Finally, the sections were viewed under a light microscope (magnification, x200; Olympus Corporation), and 10 areas were randomly selected from each slice for further analysis.

Reverse transcription-quantitative polymerase chain reaction (RT-qPCR). Prostate tissues were subjected to RT-qPCR analysis. Total RNA was extracted from the prostate tissues using TRIzol® reagent (Invitrogen; Thermo Fisher Scientific, Inc., Waltham, MA, USA) according to the manufacturer's protocols. Total RNA (1 μg) was reverse transcribed into cDNA using the PrimeScript™ RT reagent kit (Takara Bio, Inc., Otsu, Japan) according to the manufacturer's protocols. qPCR was performed using the cDNA with the SYBR-Green mix (Takara Bio, Inc.) on an ABI 7500 Real-Time PCR system (Applied Biosystems; Thermo Fisher Scientific, Inc.). All reactions were conducted in a volume of 20 μl, and the relative expression of the different genes was normalized against GAPDH. The sequences of the primers were as follows: Rat NLRP3, forward 5'-CCAGGGCTCTGTTCATTG-3', reverse, 5'-CCTTGGCTTTCACTTCG-3'; rat ASC, forward 5'-AGACATGGGCATACAGGAGC-3', reverse, 5'-GCAATGAGTGCTTGCCTGTG-3'; rat caspase-1, forward 5'-AAGAAGGTGGCGCATTTCCT-3', reverse, 5'-GACGTGTACGAGTGGGTGTT-3'; rat LC3B, forward 5'-GTCGCTAACAAGCAGTGGGA-3', reverse, 5'-AGGGCTTCTGGGGCTCTAAT-3'; rat Beclin 1, forward 5'-AGCACGCCATGTATAGCAAAGA-3', reverse, 5'-GGAAGAGGGAAAGGACAGCAT-3'; rat p62, forward 5'-GCTGCTCTCTTCAGGCTTACAG-3', reverse, 5'-CCTGCTTCACAGTAGACGAAAG-3'; and rat GAPDH, forward 5'-GGCACAGTCAAGGCTGAGAATG-3' and reverse, 5'-ATGGTGGTGAAGACGCCAGTA-3'.

The thermocycling conditions were as follows: 95˚C for 30 sec, 40 cycles of denaturation at 95˚C for 5 sec, and extension at 60˚C for 40 sec. All samples were repeated three times and the melting curves of all products were analyzed. The quantification cycle for each sample were calculated using the $2^{-\Delta\Delta Cq}$ data analysis method (20).

Western blot analysis. Isolated rat prostates were homogenized in a lysis buffer obtained from Shanghai Biyuntian Bio-Technology Co., Ltd. (Shanghai, China) with a polytron homogenizer (IKA GmbH, Königswinter, Germany) on ice. The lysates were subsequently denatured with SDS loading buffer (5X) at 100˚C for 10 min. Protein samples (40 μg) were equally loaded, which were then separated by 12% SDS-PAGE and subsequently transferred onto polyvinylidene difluoride membranes (EMD Millipore, Billerica, MA, USA). The membranes were blocked with 5% non-fat milk dissolved in Tris-buffered saline with Tween-20 (TBST) for 1 h at room temperature, and incubated with primary antibodies against GAPDH (cat. no. ab204481), NLRP3 (cat. no. ab214185), ASC (cat. no. ab47092), caspase-1 (cat. no. ab108362), Beclin 1 (cat. no. ab207612), LC3B (cat. no. ab48394), p62 (cat. no. ab91526; all at 1:2,000 dilution; Abcam), mTOR (cat. no. 2983; 1:1,000 dilution; Cell Signaling Technology, Inc., Danvers, MA, USA) and phosphorylated mTOR (p-mTOR; phosphorylated on Ser-2448) (cat. no. 2971; 1:1,000 dilution; Cell Signaling Technology, Inc.) overnight at 4˚C. Following three washes in TBST, the membranes were subsequently incubated with a secondary antibody (cat. no. C51007-08; 1:10,000 dilution; LI-COR Biosciences, Lincoln, NE, USA) conjugated to horseradish peroxidase for 1 h at room temperature. Finally, the membranes were scanned with a two-color infrared imaging system (Odyssey® Infrared Imaging system; LI-COR Biosciences). GAPDH (cat. no. ab204481; 1:2,000; Abcam) was used as the endogenous reference protein. Quantity One 4.6.2 software (Bio-Rad Laboratories, Inc., Hercules, CA, USA) was used for densitometry analysis.

Transmission electron microscopy (TEM) analysis. The isolated prostate tissues were cut into 1-mm^3 pieces and fixed in 0.1 M phosphate buffer (pH 7.4) containing 2.5% glutaraldehyde for

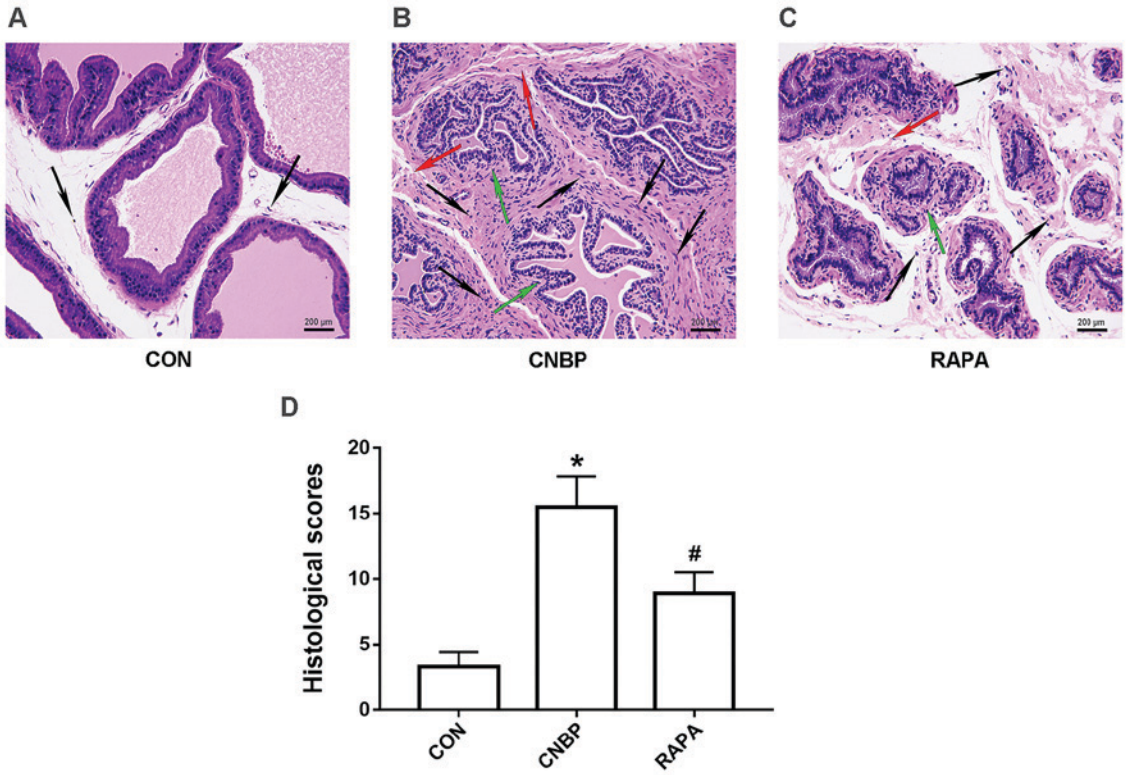

Figure 2. Histological alterations and quantitative analysis of histology of rat prostate tissues from the three groups. Representative histological images are presented, following hematoxylin and eosin staining (magnification, x200; scale bar, 200 μm) of the prostates of rats from the (A) CON, (B) CNBP, and (C) RAPA-treated groups. (D) Quantitative analysis of the histological alterations in the different groups. Data are presented as the mean ± standard deviation. The black arrows indicate inflammatory cells in the prostate tissues of the rats; the green arrows indicate glandular epithelial degeneration in the prostate tissues of the rats; the red arrows indicate the interstitial edema in the prostate tissues of the rats. *P<0.05 vs. the CON group; $^{\#}$P<0.05 vs. the CNBP group. CON, control; CNBP, chronic non-bacterial prostatitis; RAPA, rapamycin.

>3 h at 4˚C. Following three washes with phosphate buffer, the samples were stained with 1% osmium tetroxide for 1 h at 4˚C, and then dehydrated with alcohol and acetone. Subsequently, the tissues were embedded in Epon 812 resin and polymerized with pure resin at 70˚C for 24 h. The ultrathin sections (~70 nm) were obtained using an ultramicrotome (RMC Boeckeler Instruments, Inc., Tucson, AZ, USA), and subsequently stained with 5% uranyl acetate and lead citrate for 30 min at 37˚C. The sections were examined and images were captured using a transmission electron microscope (Tecnai G2 F30; FEI Co., Thermo Fisher Scientific, Inc.); five randomly selected fields from the stained tissue sections were examined (magnification, x5,000), and the number of autophagosomes in each field was counted manually.

Statistical analysis. All experiments were independently repeated three times. Data are expressed as the mean ± standard deviation. Statistical analysis was performed with one-way analysis of variance followed by a Tukey's test using SPSS software version 19.0 (IBM Corp., Armonk, NY, USA). P<0.05 was considered to indicate a statistically significant difference.

Results

Castration combined with 17β-estradiol injection causes CNBP in rats. In order to assess prostatic alterations following CNBP in the present study, H&E staining was performed to assess the histopathological changes in the prostates. A normal appearance of the glandular epithelium and stroma was noted in the prostate tissues of rats in the control group, and the acinus was filled with eosinophilic secretions; no clear indications of leukocyte infiltration were observed around the acinus (Fig. 2A). However, glandular epithelial degeneration, interstitial edema and extensive infiltration of inflammatory cells were detected in the prostate tissues of rats in the CNBP group; inflammatory cell infiltration was predominantly confined to the interstitial area, but was also observed in the glandular cavity (Fig. 2B). In addition, when compared with the CNBP group, the number of inflammatory cells infiltrating around the acinus was notably reduced in the rapamycin-treated group; the severity of glandular epithelial degeneration and interstitial edema was also reduced (Fig. 2C). Subsequent quantitative analysis supported these findings (P<0.05; Fig. 2D).

Rapamycin inhibits NLRP3 inflammasome activation in the prostates of the CNBP rats. In order to assess the degree of NLRP3 inflammasome activation in the prostate tissues of rats, IHC, RT-qPCR and western blotting were performed to measure the expression levels of NLRP3, ASC and caspase-1. The results of IHC revealed that NLRP3-positive staining was rarely observed in the control group, whereas notable NLRP3 expression was detected in the CNBP group; however, the number of cells stained positive for NLRP3 was also decreased in the rapamycin-treated group when compared with the CNBP group. Similar trends in expression were

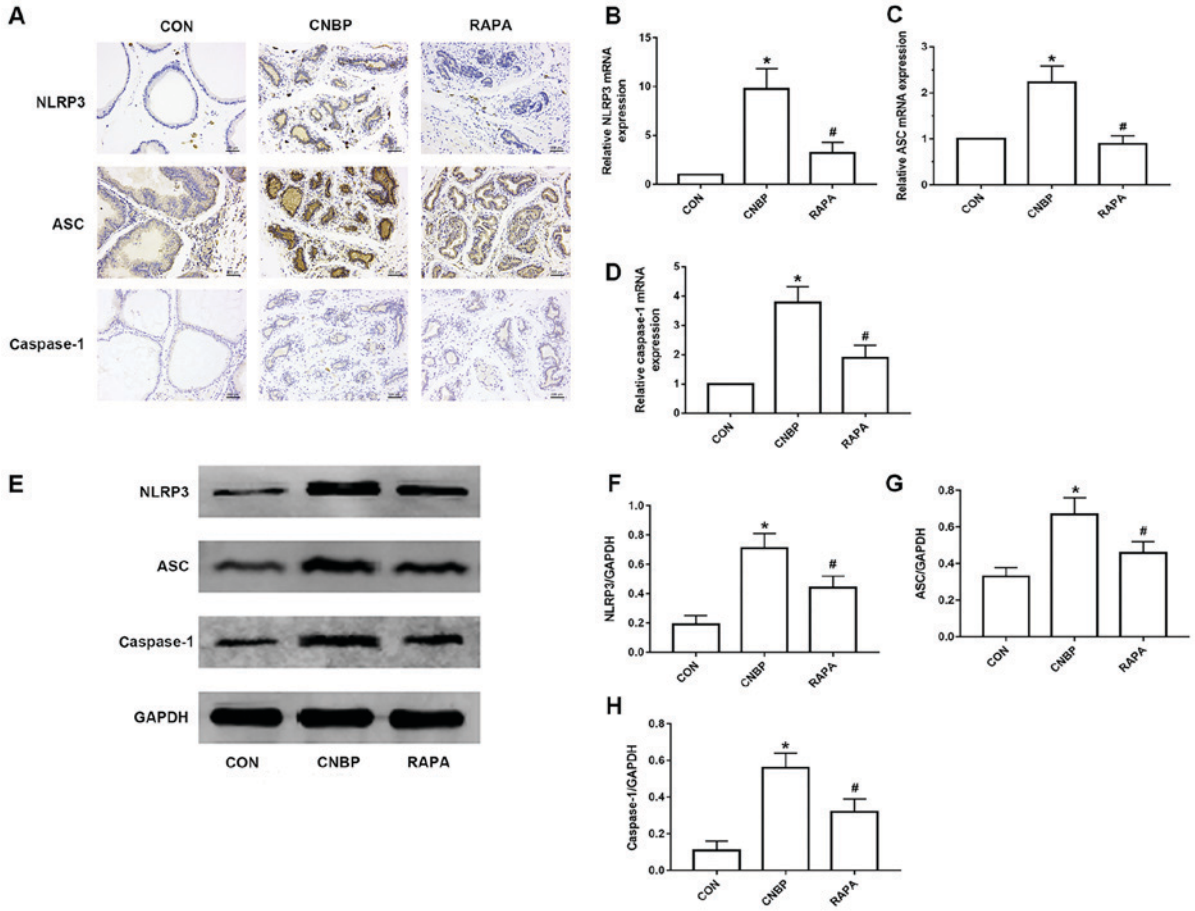

Figure 3. Rapamycin treatment reduces the upregulated expression of NLRP3, ASC and caspase-1 in the prostates of rats. (A) Representative IHC images of NLRP3, ASC and caspase-1 expression in the prostates of rats from the three groups (magnification, 200x; scale bar, 200 μm). Relative mRNA expression levels of (B) NLRP3, (C) ASC, and (D) caspase-1 in the prostates of rats from the different groups as detected by reverse transcription-quantitative polymerase chain reaction analysis. (E) Representative images of western blotting of NLRP3, ASC and caspase-1 in the different groups. Quantitative analysis was used to assess the levels of (F) NLRP3, (G) ASC and (H) caspase-1 in the different groups. The values obtained were normalized against GAPDH. Data are expressed as the mean ± standard deviation. *P<0.05 vs. the CON group; #P<0.05 vs. the CNBP group. CON, control; CNBP, chronic non-bacterial prostatitis; RAPA, rapamycin; IHC, immunohistochemistry; NLPR3, Nod-like receptor family pyrin domain-containing protein 3; ASC, apoptosis-associated speck-like protein containing a caspase recruitment domain.

noted for ASC and caspase-1 (Fig. 3A). Compared with the control group, the relative mRNA expression levels of NLRP3, ASC and caspase-1 were significantly increased in the CNBP group; however, expression was inhibited upon administration with rapamycin (P<0.05; Fig. 3B-D). In addition, the results of western blotting revealed that, compared with the control group, the protein expression levels of NLRP3, ASC and caspase-1 were significantly upregulated in the CNBP group, whereas rapamycin treatment led to a significant inhibition of NLRP3, ASC and caspase-1 protein expression compared with the CNBP group (P<0.05; Fig. 3E-H).

Rapamycin reduces the expression levels of IL-1β and IL-18 via suppressing NLRP3 inflammasome activation. In the present study, following analysis of the molecules located downstream of the NLRP3 inflammasome pathway, the concentrations of IL-1β and IL-18 in the serum of the rats from the different groups were detected using an ELISA kit. The combination of castration and 17β-estradiol treatment significantly increased the serum concentrations of IL-1β and IL-18 in the CNBP group compared with the control group, whereas rapamycin treatment led to a significant reduction in the levels of IL-1β and IL-18 compared with the CNBP group (P<0.05; Fig. 4A and B).

Rapamycin induces autophagy by inhibiting mTOR phosphorylation in CNBP rats. Considering the role of rapamycin in inducing autophagy, western blotting, RT-qPCR, IHC and TEM analyses were performed to analyze the level of autophagy in the prostate tissues of rats from the different groups. As indicated by RT-qPCR analysis, the relative mRNA expression levels of LC3B and Beclin 1 in the CNBP group were significantly decreased compared with the control group, whereas rapamycin treatment upregulated the expression of LC3B and Beclin 1 mRNA compared with the CNBP group (P<0.05; Fig. 5A and B); the expression levels of p62 were significantly upregulated in the CNBP group compared with the control; however, this was reversed in response to treatment with rapamycin (P<0.05; Fig. 5C). Western blot analysis demonstrated that, compared with the control group, the protein expression levels of LC3B-II and Beclin 1 were also significantly decreased in the CNBP group, but were significantly increased in the rapamycin-treated group compared with the CNBP group (P<0.05; Fig. 5D-F). Additionally,

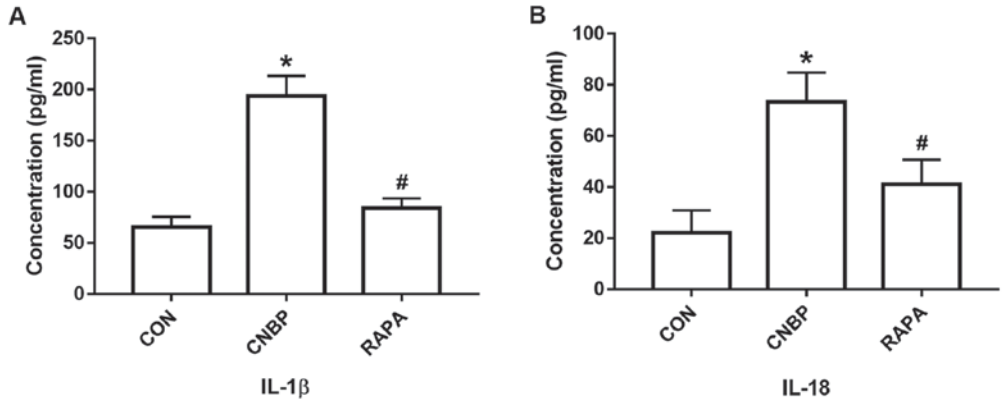

Figure 4. Levels of serum IL-1β and IL-18 in rats from different groups. The serum concentrations of (A) IL-1β and (B) IL-18, as revealed by ELISA, in rats from the three groups. Data are expressed as the mean ± standard deviation. *P<0.05 vs. the CON group; #P<0.05 vs. the CNBP group. IL, interleukin; CON, control; CNBP, chronic non-bacterial prostatitis; RAPA, rapamycin; ELISA, enzyme-linked immunosorbent assay.

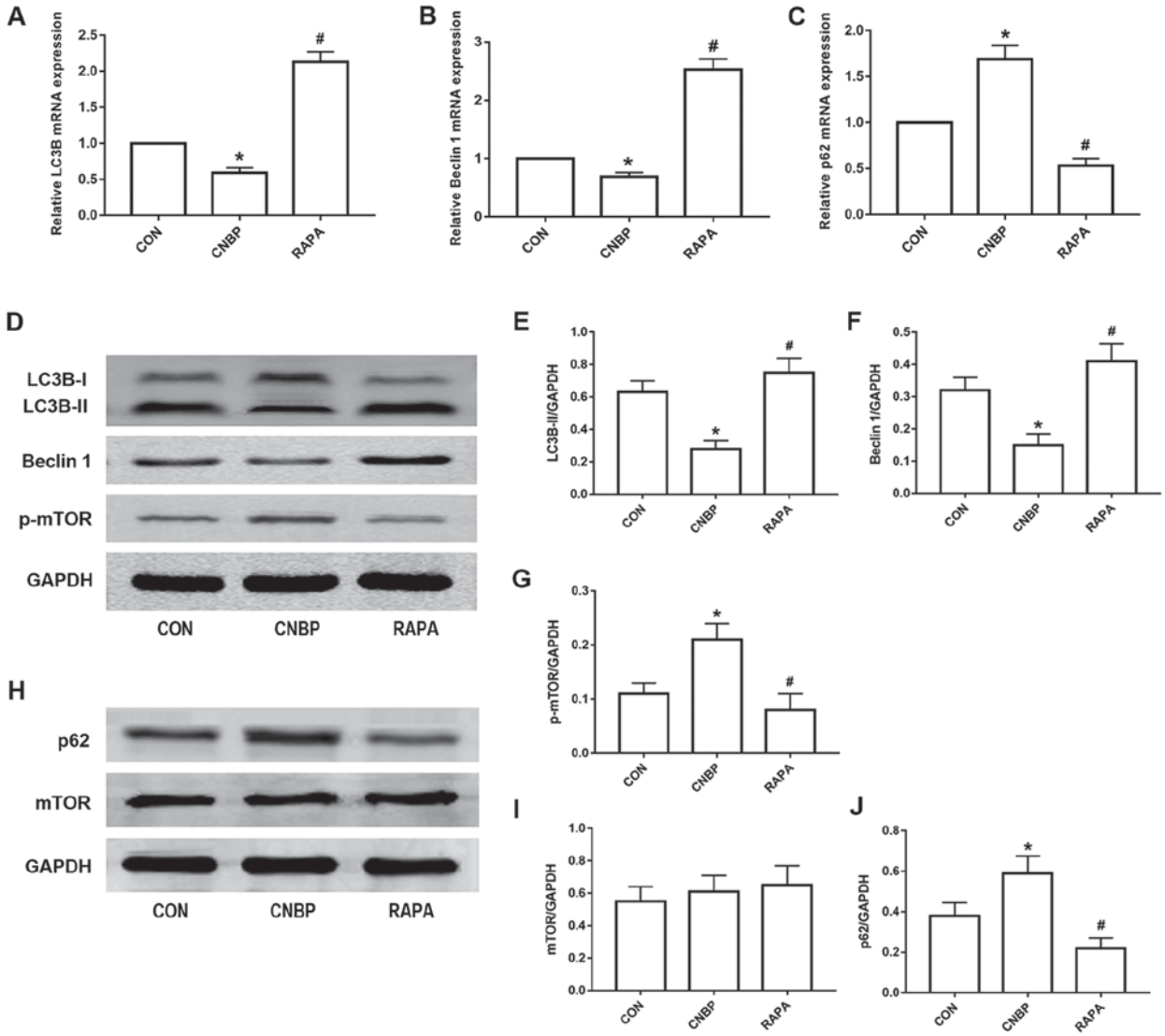

Figure 5. Rapamycin treatment induces autophagy in rats via the inhibition of mTOR phosphorylation. The relative mRNA expression levels of (A) LC3B, (B) Beclin 1, and (C) p62, as measured by reverse transcription-quantitative polymerase chain reaction analysis, in the prostates of rats from the three groups. (D) Representative western blot images of LC3B, Beclin 1 and p-mTOR from the three groups. Quantitative analysis was used to assess the levels of (E) LC3B-II, (F) Beclin 1, and (G) p-mTOR in the different groups. (H) Representative western blot images of p62 and mTOR from the three groups. Quantitative analysis was used to assess the expression levels of (I) p62 and (J) mTOR in the different groups. The values obtained were normalized against GAPDH. Data are expressed as the mean ± standard deviation. *P<0.05 vs. the CON group; #P<0.05 vs. the CNBP group. CON, control; CNBP, chronic non-bacterial prostatitis; RAPA, rapamycin; mTOR, mammalian target of rapamycin; p-mTOR, phosphorylated mTOR; LC3B, microtubule-associated protein 1 light chain 3β.

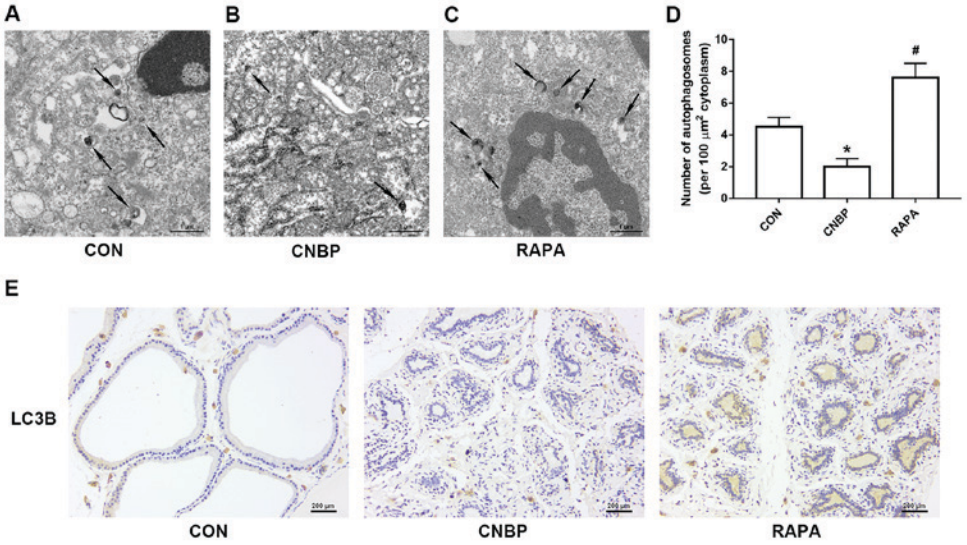

Figure 6. Ultrastructural alterations due to autophagy and cells positively stained for LC3B in rats of the three different groups, as detected by TEM and IHC analyses. Representative TEM images of autophagosomes in the (A) CON, (B) CNBP and (C) RAPA groups (magnification, x5,000; scale bar, 1 μm). The black arrows indicate autophagosomes with a double membrane in the prostates of rats. (D) Quantitative analysis of autophagosomes in the different groups. (E) Representative IHC images of LC3B in the three groups (magnification, x200; scale bar, 200 μm). Data are expressed as the mean ± standard deviation. *P<0.05 vs. the CON group; #P<0.05 vs. the CNBP group. CON, control; CNBP, chronic non-bacterial prostatitis; RAPA, rapamycin; TEM, transmission electron microscopy; IHC, immunohistochemistry; LC3B, microtubule-associated protein 1 light chain 3β.

compared with the control group, the protein expression levels of p-mTOR in the prostate of the CNBP rats were significantly increased (P<0.05; Fig. 5D and G), whereas rapamycin treatment significantly suppressed the upregulated levels of p-mTOR (P<0.05). In addition, the protein expression levels of mTOR in the prostate tissues of rats in the three groups did not indicate any significant differences (Fig. 5H and I); however, western blot analysis of p62, a marker of autophagosomal degradation, revealed an expression profile contrary to that of LC3B-II and Beclin 1 (Fig. 5H and J).

Examination of the autophagosomes and LC3B-positive staining of cells are the techniques considered to be the 'gold standard' to identify autophagy (21). Therefore, TEM analysis was used to observe cellular autophagy at the ultrastructural level in the present study. Autophagic vacuoles with a double membrane were observed in the control group (Fig. 6A), but fewer were detected in the CNBP group (Fig. 6B). Conversely, numerous autophagosomes were observed in the rapamycin-treated group (Fig. 6C). Quantitative analysis of these results also supported these findings (P<0.05; Fig. 6D). Similarly, the results of IHC revealed that, compared with the control group, the number of cells positively stained for LC3B were notably decreased in the CNBP group; however, a marked increase in the number of LC3B-positive cells was reported in the rapamycin-treated group compared with the CNBP group (Fig. 6E).

Discussion

CNBP is a very common disease encountered in urological clinics, and is associated with male infertility, sexual dysfunction, BPH and prostate cancer (6-8); however, the etiology of CNBP is yet to be elucidated. To investigate the underlying mechanisms of CNBP, numerous experimental animal models that mimic human category III prostatitis (CP) have been developed by immune manipulation (22), infection (23), or hormonal treatment (24,25). Therefore, one possible mechanism that may, at least in part, be responsible for the pathogenesis of CNBP is sex hormone imbalance. It has been reported that the increased prevalence of CNBP is associated with a decrease in the testosterone (T) to estrogen (E2) ratio in the serum (26), which was due to the decreased anti-inflammatory effect of T, as well as an increased proinflammatory function of E2 (26). Therefore, hormone imbalance may induce prostatic inflammation when the concentration of androgen decreases and/or the E2 concentration remains unchanged or increases. Administration of exogenous 17β-estradiol to old (10-13 months) male Wistar rats led to a 3.7-fold increase in the incidence of CNBP and a 2- to 6-fold increase in the severity of prostate inflammation (24). Castration was also reported to have a similar effect (24); combined with estradiol injection, castration was also used to establish a model of CP in Wistar rats (27). Additionally, Keith *et al* (28) reported that Wistar rats tend to develop spontaneous prostatitis, which may have a serious impact on the accuracy of the experimental results obtained. To the best of our knowledge, spontaneous prostatitis has not been reported in Sprague-Dawley rats, and providing that this is the case, Sprague-Dawley rats may be used to build a CNBP model less prone to these types of experimental error. Thus, Sprague-Dawley rats, rather than Wistar rats, were selected to establish the CNBP model in the present study. Although castration alone is able to induce prostatic inflammation (24), it has been reported that the combination of castration and estrogen injection induced markedly severe prostatitis and pathological changes (25). Furthermore, it has been confirmed that the ratio of T to E2 is negatively correlated with the majority of inflammatory markers (29), which indicates that combining castration with E2 injection may provide a more stable approach to establishing the CNBP model. Therefore, in the present study, the mechanism

underlying the pathogenesis of CNBP was investigated using a rat model induced by castration and 17β-estradiol injection. In the present study, prostatic interstitial edema and infiltration of numerous inflammatory cells around the acinar cavity were observed in the prostate tissues of CNBP rats upon H&E staining. Furthermore, varying degrees of tissue damage in the prostate lumens were also observed in the CNBP rats. These results indicated that the combination of castration and 17β-estradiol injection may have induced inflammation in the prostates of rats.

It is well-known that the NLRP3 inflammasome and its downstream molecules, IL-1β and IL-18, are closely associated with the pathogenesis of chronic inflammatory diseases, including cryopyrin-associated periodic syndrome (CAPS), inflammatory bowel disease (IBD) and type 2 diabetes (30). Jiang *et al* (31) have demonstrated that the NLRP3 inflammasome is activated in CAPS, and inhibition of the NLRP3 inflammasome exerted significant therapeutic effects against this condition. The NLRP3 inflammasome, which is composed of NLRP3, ASC and caspase-1, is usually activated in monocytes and macrophages; it was originally described as a cytosolic multiprotein structure of the innate immune system (9). The stimulation of DAMPs or PAMPs, including lipopolysaccharide and other molecules derived from cellular damage processes, promotes the activation of inflammasomes, thereby leading to the activation of caspase-1; activated caspase-1 ultimately transforms the endogenous proinflammatory cytokines, IL-1β and IL-18, into their mature secreted forms (10). Collectively, activation of the NLRP3 inflammasome may serve an important role in the maturation and release of inflammatory cytokines, particularly IL-1β and IL-18. It is well established that IL-1β and IL-18 are two important cytokines involved in the inflammatory response, which fulfill critical roles in various diseases associated with infection, injury, and antigenic stimulation (32). Vincent and Mohr (33) reported that IL-1β increased tissue injury via nuclear factor-κB activation and leukocyte adhesion. Park *et al* (34) reported that elevated levels of IL-18 were associated with severe lupus nephritis in patients with systemic lupus erythematous. Furthermore, activated NLRP3 inflammasome was detected in patients with IBD and myelodysplastic syndromes (35,36). Therefore, activation of the NLRP3 inflammasome is a critical step in various inflammatory responses. In the present study, via IHC, RT-qPCR and western blot analyses, it was demonstrated that the expression levels of NLRP3, ASC and caspase-1 in the prostate tissues of CNBP rats were significantly increased compared with in the control group. Furthermore, the serum levels of IL-1β and IL-18 detected by ELISA were also increased in the CNBP group. These results indicated that the NLRP3 inflammasome was activated in the prostate tissues of the CNBP rats, and the activated NLRP3 inflammasome, together with the increased expression levels of IL-1β and IL-18, may contribute to the inflammatory cell infiltration and histological changes observed in the prostates of CNBP rats.

Autophagy is an important cellular homeostatic process by which cells degrade damaged or senescent components. This process involves a variety of autophagy-associated proteins, of which Beclin 1, LC3 and p62 serve crucial roles (37-39). Beclin 1 is involved in the formation of autophagosomes; p62 serves an important role in the process of autophagosomal degradation (37). LC3 fulfills critical roles in the maturation of autophagosomes and the formation of autolysosomes (38). LC3 exists in the form of LC3-I under normal conditions, but may be converted into LC3-II by covalent association with the lipid phosphatidylethanolamine on autophagosomal membranes during maturation (38,39). At present, LC3-II is the only well-characterized protein that is specifically localized to autophagic structures throughout the process of phagophore formation to lysosomal degradation (40). It should be noted that LC3 is expressed as three isoforms in mammalian cells, LC3A, LC3B and LC3C; however, only LC3B-II correlates with an increased number of autophagic vesicles (41). As LC3-II tends to have a higher affinity to its antibody than LC3-I, comparisons of LC3-I expression, or the LC3-I/LC3-II ratio may lead to numerous false-positive or false-negative results (42). Therefore, LC3B, Beclin 1 and p62 have been considered to be specific markers that may be used to monitor cellular autophagy. The process of autophagy eliminates senescent organelles and abnormal cytosolic macromolecules under physiological conditions; however, autophagy may contribute to the pathogenesis of various diseases (43). For example, autophagy impairment has been reported to induce the abnormal accumulation of mutant proteins in Alzheimer's disease (44). Ehrnhoefer *et al* (45) demonstrated that the dysfunction of autophagy promoted an accumulation of mutant huntingtin in Huntington's disease. Recently, increasing evidence has indicated that autophagy may be regulated by E2; for example, it was revealed that E2 functions as a negative regulator of autophagy in the uterus of ovariectomized mice, and the inhibition of autophagy by E2 was mediated via mTOR signaling (46). Wang *et al* (47) demonstrated that E2 protected cardiomyocytes against damage induced by lipopolysaccharide via autophagy inhibition. Fu *et al* (48) demonstrated that E2 suppressed autophagy in osteocyte-like MLO-Y4 cells and that this effect was reversed by rapamycin. Therefore, based on the aforementioned studies, the present study proposed that E2 may promote the progression of CNBP by inhibiting autophagy. The results of the present study indicated that the level of autophagy, as reflected by the levels of LC3B (a more common isoform of LC3), Beclin 1 and autophagosome abundance, were significantly suppressed in the prostate tissues of rats in the CNBP group compared with the control group. Conversely, as a specific marker of autophagosomal degradation (21), p62 exhibited an expression profile contrary to that of LC3B and Beclin 1.

In addition, accumulating evidence has demonstrated an association between the NLRP3 inflammasome and autophagy. Autophagy has been reported to exert numerous effects on regulating inflammasome activation, including eliminating endogenous signals that activate the inflammasome, and degrading inflammasome components. In particular, it has been reported that the suppression of autophagy promoted NLRP3 inflammasome activation, and the subsequent release of IL-1β and IL-18 (49). The impairment of autophagy in macrophages was demonstrated to promote NLRP3 inflammasome activation and lead to the hypersecretion of IL-1β (15). X-11-5-27, a daidzein derivative, attenuated activation of the

NLRP3 inflammasome by promoting autophagy in acute monocytic leukemia (50). Therefore, on the basis of these findings, the present study proposed that the suppression of autophagy may contribute to the progression of CNBP via activation of the NLRP3 inflammasome. In the present study, it was reported that the expression levels of IL-1β and IL-18 in rats of the CNBP group were significantly increased compared with in the control group. Similarly, the expression levels of the NLRP3 inflammasome components, NLRP3, ASC and caspase-1, were also significantly increased in the CNBP group compared with the control group. Collectively, these findings indicated that E2 promoted the progression of chronic inflammation in the prostate tissues by inhibiting autophagy. This process may be associated with activation of the NLRP3 inflammasome and its downstream molecules, including IL-1β and IL-18.

To further investigate the role of autophagy in CNBP, rapamycin, a well-known specific inducer of autophagy that negatively regulates mTOR (51), was used to induce autophagy in rats with CNBP. Firstly, via western blotting, IHC and RT-qPCR analyses, it was demonstrated that, compared with the CNBP group, rapamycin treatment significantly increased the levels of autophagy-associated markers, including LC3B and Beclin 1 in the prostate tissues of rats; rapamycin induced autophagy in the prostates of rats by inhibiting the phosphorylation of mTOR. TEM analysis also demonstrated that rapamycin significantly promoted the formation of autophagosomes compared with the CNBP group. In addition, the present study revealed that rapamycin treatment notably attenuated inflammatory cell infiltration, glandular epithelial degeneration and interstitial edema in the prostates of the CNBP rats, and rapamycin treatment was also reported to significantly suppress the upregulated expression of NLRP3 inflammasome-associated components, and reduced the levels of IL-1β and IL-18 in rats of the CNBP group as detected by IHC, RT-qPCR, western blotting and ELISA analyses. Collectively, the findings of the present findings indicated that the combination of castration and 17β-estradiol injection induced a hormone imbalance-induced, NLRP3 inflammasome-mediated chronic inflammatory response in the prostates of rats via the inhibition of autophagy, a phenomenon that could be reversed by rapamycin treatment. However, there was a limitation of the present study. The size of prostates from the CNBP rats were notably smaller and the parenchyma of these prostates were decreased when compared with the control group.

In conclusion, the present study reported that the imbalance in sex hormones induced by castration and 17β-estradiol injection promoted inflammation in the prostates of rats. Furthermore, it was demonstrated that rapamycin alleviated the chronic inflammatory response in the prostate tissues of rats via the induction of autophagy and inhibiting the activation of the NLRP3 inflammasome, as suggested by alterations in the expression levels of IL-1β and IL-18. The findings of present study may not only improve understanding of the mechanism underlying the pathogenesis of sex hormone imbalance-induced CNBP, but also provides a potential therapeutic target for clinicians; however, further investigation is required to determine the molecular pathways by which autophagy affects the progression of CNBP.

Acknowledgements

Not applicable.

Funding

The present study was supported by the National Natural Science Foundation of China (grant nos. 81470923, 81470986, 81770078 and 81770688).

Availability of data and materials

The data and materials used or analyzed during this study are available from the corresponding author on reasonable request.

Authors' contributions

XC and JZ contributed to the design of the study, and critically revised the manuscript for important intellectual content. JL and YS designed the study, performed the experiments and collected the experimental data. JL drafted this paper. YC, PL and FL helped to perform experiments and analyze the experimental data.

Ethics approval and consent to participate

The present study was approved by the Ethical Committee on Animal Experiments at Renmin Hospital of Wuhan University (approval no. WDRM-20170709).

Patient consent for publication

Not applicable.

Competing interests

The authors declare that they have no competing interests.

References

1. Ellem SJ, Wang H, Poutanen M and Risbridger GP: Increased endogenous estrogen synthesis leads to the sequential induction of prostatic inflammation (prostatitis) and prostatic pre-malignancy. Am J Pathol 175: 1187-1199, 2009.
2. Krieger JN, Lee SW, Jeon J, Cheah PY, Liong ML and Riley DE: Epidemiology of prostatitis. Int J Antimicrob Agents 31 (Suppl 1): S85-S90, 2008.
3. Vykhovanets EV, Resnick MI, MacLennan GT and Gupta S: Experimental rodent models of prostatitis: Limitations and potential. Prostate Cancer Prostatic Dis 10: 15-29, 2007.
4. Krieger JN, Nyberg L Jr and Nickel JC: NIH consensus definition and classification of prostatitis. JAMA 282: 236-237, 1999.
5. McNaughton Collins M, MacDonald R and Wilt TJ: Diagnosis and treatment of chronic abacterial prostatitis: A systematic review. Ann Intern Med 133: 367-381, 2000.
6. Hao ZY, Li HJ, Wang ZP, Xing JP, Hu WL, Zhang TF, Zhang XS, Zhou J, Tai S and Liang CZ: The prevalence of erectile dysfunction and its relation to chronic prostatitis in Chinese men. J Androl 32: 496-501, 2011.
7. Delongchamps NB, de la Roza G, Chandan V, Jones R, Sunheimer R, Threatte G, Jumbelic M and Haas GP: Evaluation of prostatitis in autopsied prostates-is chronic inflammation more associated with benign prostatic hyperplasia or cancer? J Urol 179: 1736-1740, 2008.
8. Sfanos KS and De Marzo AM: Prostate cancer and inflammation: The evidence. Histopathology 60: 199-215, 2012.

9. Schroder K and Tschopp J: The inflammasomes. Cell 140: 821-832, 2010.
10. Jo EK, Kim JK, Shin DM and Sasakawa C: Molecular mechanisms regulating NLRP3 inflammasome activation. Cell Mol Immunol 13: 148-159, 2016.
11. Strowig T, Henao-Mejia J, Elinav E and Flavell R: Inflammasomes in health and disease. Nature 481: 278-286, 2012.
12. Deretic V: Autophagy in infection. Curr Opin Cell Biol 22: 252-262, 2010.
13. He C and Klionsky DJ: Regulation mechanisms and signaling pathways of autophagy. Annu Rev Genet 43: 67-93, 2009.
14. Kroemer G, Mariño G and Levine B: Autophagy and the integrated stress response. Mol Cell 40: 280-293, 2010.
15. Harris J, Hartman M, Roche C, Zeng SG, O'Shea A, Sharp FA, Lambe EM, Creagh EM, Golenbock DT, Tschopp J, *et al*: Autophagy controls IL-1beta secretion by targeting pro-IL-1beta for degradation. J Biol Chem 286: 9587-9597, 2011.
16. Saitoh T, Fujita N, Jang MH, Uematsu S, Yang BG, Satoh T, Omori H, Noda T, Yamamoto N, Komatsu M, *et al*: Loss of the autophagy protein Atg16L1 enhances endotoxin-induced IL-1beta production. Nature 456: 264-268, 2008.
17. Su Y, Lu J, Chen X, Liang C, Luo P, Qin C and Zhang J: Rapamycin alleviates hormone imbalance-induced chronic nonbacterial inflammation in rat prostate through activating autophagy via the mTOR/ULK1/ATG13 signaling pathway. Inflammation 41: 1384-1395, 2018.
18. Liu RF, Fu G, Li J, Yang YF, Wang XG, Bai PD and Chen YD: Roles of autophagy in androgen-induced benign prostatic hyperplasia in castrated rats. Exp Ther Med 15: 2703-2710, 2018.
19. Meng Y, Pan M, Zheng B, Chen Y, Li W, Yang Q, Zheng Z, Sun N, Zhang Y and Li X: Autophagy attenuates angiotensin ii-induced pulmonary fibrosis by inhibiting redox imbalance-mediated NOD-like receptor family pyrin domain containing 3 inflammasome activation. Antioxid Redox Signal: May 7, 2018 (Epub ahead of print).
20. Livak KJ and Schmittgen TD: Analysis of relative gene expression data using real-time quantitative PCR and the 2(-Delta Delta C(T)) method. Methods 25: 402-408, 2001.
21. Klionsky DJ, Abeliovich H, Agostinis P, Agrawal DK, Aliev G, Askew DS, Baba M, Baehrecke EH, Bahr BA, Ballabio A, *et al*: Guidelines for the use and interpretation of assays for monitoring autophagy in higher eukaryotes. Autophagy 4: 151-175, 2008.
22. Liu KJ, Chatta GS, Twardzik DR, Vedvick TS, True LD, Spies AG and Cheever MA: Identification of rat prostatic steroid-binding protein as a target antigen of experimental autoimmune prostatitis: Implications for prostate cancer therapy. J Immunol 159: 472-480, 1997.
23. Kaplan L, Lee C and Schaeffer AJ: Effect of castration on experimental bacterial prostatitis in rats. Prostate 4: 625-630, 1983.
24. Naslund MJ, Strandberg JD and Coffey DS: The role of androgens and estrogens in the pathogenesis of experimental nonbacterial prostatitis. J Urol 140: 1049-1053, 1988.
25. Robinette CL: Sex-hormone-induced inflammation and fibromuscular proliferation in the rat lateral prostate. Prostate 12: 271-286, 1988.
26. Bernoulli J, Yatkin E, Konkol Y, Talvitie EM, Santti R and Streng T: Prostatic inflammation and obstructive voiding in the adult Noble rat: Impact of the testosterone to estradiol ratio in serum. Prostate 68: 1296-1306, 2008.
27. Kamijo T, Sato S and Kitamura T: Effect of cernitin pollen-extract on experimental nonbacterial prostatitis in rats. Prostate 49: 122-131, 2001.
28. Keith IM, Jin J, Neal D Jr, Teunissen BD and Moon TD: Cell relationship in a Wistar rat model of spontaneous prostatitis. J Urol 166: 323-328, 2001.
29. Jia YL, Liu X, Yan JY, Chong LM, Li L, Ma AC, Zhou L and Sun ZY: The alteration of inflammatory markers and apoptosis on chronic prostatitis induced by estrogen and androgen. Int Urol Nephrol 47: 39-46, 2015.
30. Ozaki E, Campbell M and Doyle SL: Targeting the NLRP3 inflammasome in chronic inflammatory diseases: Current perspectives. J Inflamm Res 8: 15-27, 2015.
31. Jiang H, He H, Chen Y, Huang W, Cheng J, Ye J, Wang A, Tao J, Wang C, Liu Q, *et al*: Identification of a selective and direct NLRP3 inhibitor to treat inflammatory disorders. J Exp Med 214: 3219-3238, 2017.
32. Broz P and Monack DM: Molecular mechanisms of inflammasome activation during microbial infections. Immunol Rev 243: 174-190, 2011.
33. Vincent JA and Mohr S: Inhibition of caspase-1/interleukin-1beta signaling prevents degeneration of retinal capillaries in diabetes and galactosemia. Diabetes 56: 224-230, 2007.
34. Park MC, Park YB and Lee SK: Elevated interleukin-18 levels correlated with disease activity in systemic lupus erythematosus. Clin Rheumatol 23: 225-229, 2004.
35. Kanneganti TD: Inflammatory bowel disease and the NLRP3 inflammasome. N Engl J Med 377: 694-696, 2017.
36. Basiorka AA, McGraw KL, Abbas-Aghababazadeh F, McLemore AF, Vincelette ND, Ward GA, Eksioglu EA, Sallman DA, Ali NA, Padron E, *et al*: Assessment of ASC specks as a putative biomarker of pyroptosis in myelodysplastic syndromes: An observational cohort study. Lancet Haematol 5: e393-e402, 2018.
37. Wirawan E, Lippens S, Vanden Berghe T, Romagnoli A, Fimia GM, Piacentini M and Vandenabeele P: Beclin1: A role in membrane dynamics and beyond. Autophagy 8: 6-17, 2012.
38. Levine B and Kroemer G: Autophagy in the pathogenesis of disease. Cell 132: 27-42, 2008.
39. Mizushima N, Levine B, Cuervo AM and Klionsky DJ: Autophagy fights disease through cellular self-digestion. Nature 451: 1069-1075, 2008.
40. Nakatogawa H, Suzuki K, Kamada Y and Ohsumi Y: Dynamics and diversity in autophagy mechanisms: Lessons from yeast. Nat Rev Mol Cell Biol 10: 458-467, 2009.
41. Mizushima N and Yoshimori T: How to interpret LC3 immunoblotting. Autophagy 3: 542-545, 2007.
42. Barth S, Glick D and Macleod KF: Autophagy: Assays and artifacts. J Pathol 221: 117-124, 2010.
43. Kroemer G: Autophagy: A druggable process that is deregulated in aging and human disease. J Clin Invest 125: 1-4, 2015.
44. Nilsson P and Saido TC: Dual roles for autophagy: Degradation and secretion of Alzheimer's disease Aβ peptide. Bioessays 36: 570-578, 2014.
45. Ehrnhoefer DE, Martin DDO, Schmidt ME, Qiu X, Ladha S, Caron NS, Skotte NH, Nguyen YTN, Vaid K, Southwell AL, *et al*: Preventing mutant huntingtin proteolysis and intermittent fasting promote autophagy in models of Huntington disease. Acta Neuropathol Commun 6: 16, 2018.
46. Choi S, Shin H, Song H and Lim HJ: Suppression of autophagic activation in the mouse uterus by estrogen and progesterone. J Endocrinol 221: 39-50, 2014.
47. Wang F, Xiao J, Shen Y, Yao F and Chen Y: Estrogen protects cardiomyocytes against lipopolysaccharide by inhibiting autophagy. Mol Med Rep 10: 1509-1512, 2014.
48. Fu J, Hao L, Tian Y, Liu Y, Gu Y and Wu J: miR-199a-3p is involved in estrogen-mediated autophagy through the IGF-1/mTOR pathway in osteocyte-like MLO-Y4 cells. J Cell Physiol 233: 2292-2303, 2018.
49. Harris J, Lang T, Thomas JPW, Sukkar MB, Nabar NR and Kehrl JH: Autophagy and inflammasomes. Mol Immunol 86: 10-15, 2017.
50. Zhou W, Liu X, Cheng K, Zhang X, Lu J and Hu R: X-11-5-27, a daidzein derivative, inhibits NLRP3 inflammasome activity via promoting autophagy. Exp Cell Res 360: 320-327, 2017.
51. Song Y, Xue H, Liu TT, Liu JM and Chen D: Rapamycin plays a neuroprotective effect after spinal cord injury via anti-inflammatory effects. J Biochem Mol Toxicol 29: 29-34, 2015.